

Spectroscopic Evidence for Sum Frequency of Forward and Backscattered Light in Laser Plasmas

A. Giulietti, D. Giulietti,^(a) D. Batani,^(a) V. Biancalana,^(a) L. Gizzi,^(a) L. Nocera, and E. Schifano^(a)

Istituto di Fisica Atomica e Molecolare, via del Giardino, 7 56100 Pisa, Italy

(Received 11 May 1989)

Spectra of 90° scattered light from underdense plasmas show a line close to the second harmonic of laser frequency whose red shift is consistent with frequency sum between the incident laser light and Brillouin backscattered light. Time-resolved spectra give information on the dynamics of the process.

PACS numbers: 52.50.Jm, 52.40.Db

Second-harmonic generation from laser-produced plasmas have been under investigation for a long time as an important diagnostic tool of laser plasma interaction. Most of the observations and measurements have been performed in the presence of the critical layer [where $n_e = n_c = (m_e/4\pi e^2)\omega_0^2$, ω_0 being the laser frequency] in the plasma.¹⁻³ In this layer several processes (like resonance absorption and parametric decay instability) can generate ω_0 plasmons and give rise to 2ω emission. The coalescence of a resonant plasmon with another plasmon or a laser photon can also originate second-harmonic emission at 90° to the laser beam axis near the critical density.^{4,5} Only a few works report on the observation of 2ω emission from underdense plasmas. In one of them this emission was detected from a laser plasma produced in gas at electron density $n_e \approx n_c/100$.⁶ Under this condition no emission was detected at 90°, but only in the direction of the laser beam in a small solid angle.⁷ From underdense regions of plasma produced on solid targets, 90° emission of 2ω light was observed in the presence of filamentation.^{8,9}

A theory was also introduced to account for 2ω emission normal to the filament or, in a general case, normal to the laser beam. The main point was that this kind of emission requires the existence of reflected or backscattered light at $\omega_B \approx \omega_0$ in addition to the incident laser light. From this point of view we can more properly speak of "sum frequency generation" rather than second-harmonic generation. The most probable source of backscatter in an underdense plasma is stimulated Brillouin scattering (SBS). From this assumption the red shift of the Brillouin light, due to energy released to the ion-acoustic wave, was expected to produce a shift also in the "harmonic" $\omega_0 + \omega_B$ radiated normally. Unfortunately the authors were not equipped to measure such a shift.⁹

In this Letter we present time-resolved spectra at 2ω , obtained at 90° to the beam axis from a plasma produced by laser irradiation of a thin plastic film, whose spectroscopic features are consistent with the above-mentioned theory. The plastic used for thin-target preparation was polyvinyl formal and the target thickness used in the experiment was in the range 0.3–1.8 μm . The thin film was irradiated at 10640-Å laser wave-

length with a pulse of 3-ns FWHM at an irradiance up to $5 \times 10^{13} \text{ W cm}^{-2}$. The laser beam was focused perpendicularly to the target plane with an $f/8$ optics. The laser bandwidth was 0.7 Å. Second-harmonic emission at 90° (parallel to the target plane) was observed in a wide range of target thickness, down to 0.5 μm .

No 2ω emission was detected in the presence of pre-lasing, due to the early formation and expansion of the plasma. The contrast ratio (prepulse to main pulse energy ratio) was $\eta \sim 10^{-4}$. The irradiance threshold of the process was found to be of the order of $10^{12} \text{ W cm}^{-2}$ with no clear dependence on the target thickness. Only the duration of the 2ω emission was observed to decrease with decreasing target thickness, from about 2 ns for thickness above 1 μm , down to less than 100 ps at 0.5 μm . The 2ω emission showed a spiky structure in time with a poor reproducibility shot by shot. This behavior originated from the time modulations already present in the laser pulse, strongly enhanced in turn by the non-linear character of the process. The radiation emitted at 90° was collected with an $f/7$ optics, time resolved with an intensified optical streak camera, and analyzed in two different ways.

(a) *Time-resolved spectra.*—The light was first sent to an $\frac{1}{4}$ -m spectrometer with a dispersion of 34 Å/mm; the output plane of the spectrometer was imaged on the streak-camera slit. In this way, we obtained time-resolved spectra on a photographic film put on the intensifier screen. The actual dispersion on the film was carefully calibrated using the 5330-, 5341-, and 5400-Å lines of Ne. A wavelength fiducial was obtained, putting a thin wire on the spectrometer output plane perpendicular to the dispersion axis. The position of the wire was in turn calibrated with the same spectral lines.

(b) *Time-resolved images.*—In this case the image of the plasma was directly formed on the streak-camera slit after passing through a narrow-band (30 Å) interference filter centered at 5320 Å. The streak-camera slit was perpendicular to the target plane and its width was comparable with the diameter of the focal spot image. In this way, we could estimate the dimension of the region emitting 2ω light.

Figure 1 shows three time-resolved spectra. The overall duration of the emission for a target thickness of

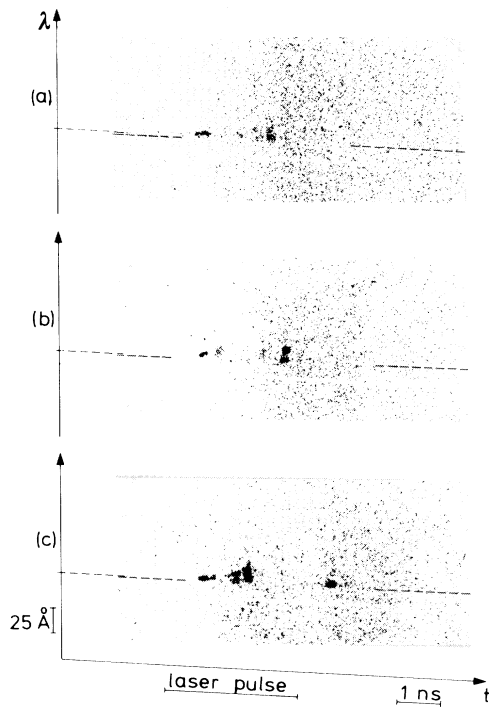


FIG. 1. Time-resolved spectra of 2ω emission. (a) Shot No. 211207: Intensity $I=1.2 \times 10^{13}$ W/cm 2 , target thickness $d=1.58$ μ m; (b) No. 211209: $I=1.4 \times 10^{13}$ W/cm 2 , $d=1.58$ μ m; (c) No. 231204: $I=1.5 \times 10^{13}$ W/cm 2 , $d=1.50$ μ m. Contrast was enhanced by photographic processing to evidence structures. The "laser pulse" bar refers to the FWHM duration and roughly matches the pulse timing. Dashed lines indicate the wavelength position of the exact $2\omega_0$.

1.5 μ m was about 2 ns. The spiky behavior of the emission, as well as its poor reproducibility, is apparent. Nevertheless, all the spectra showed the same features, namely, (1) red shift with respect to the exact second-harmonic wavelength 5320 \AA , (2) shift and bandwidth both increasing in time, (3) late-time spikes often showing doublet structure. In a small number of shots, a very late emission (during the tail of the pulse) was observed as in picture (c).

Figure 2 shows four typical time-resolved images of the second-harmonic sources in the interaction region. The extension of the emitting region perpendicular to the target plane was found to vary from spike to spike ranging from a few hundred μ m to about 1 mm. Spatial modulations parallel to the target plane in the 2ω emissivity can be also observed in most of the spikes. The origin of these modulations is still under investigation.

From the extension of the emitting region we can evaluate that the electron density was always well below the critical density. This evaluation also agrees with calculation of the electron density at the peak of the laser pulse using a self-similar model¹⁰ confirmed by simula-

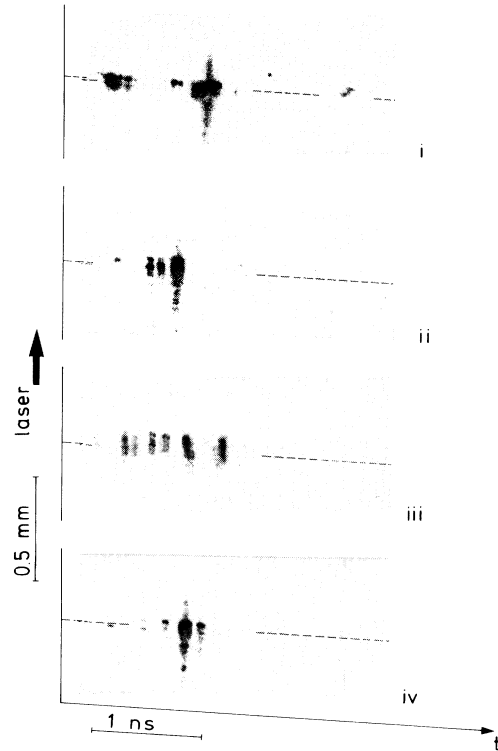


FIG. 2. Time-resolved images of 2ω sources. (i) No. 070202: $I=1.3 \times 10^{13}$ W/cm 2 , $d=1.56$ μ m; (ii) No. 060204: $I=1.5 \times 10^{13}$ W/cm 2 , $d=1.39$ μ m; (iii) No. 060209: $I=1.5 \times 10^{13}$ W/cm 2 , $d=1.39$ μ m; (iv) No. 211209: $I=1.7 \times 10^{13}$ W/cm 2 , $d=1.21$ μ m. Contrast was enhanced by photographic processing to show structures. The initial target plane position is approximately indicated by dashed lines.

tions. The contribution of processes occurring in the critical region can thus be excluded.

According to theory⁹ the 2ω emission at 90° in an underdense plasma originates from the current component $J_{2\omega}$, the part of $J_{2\omega}^{\text{ot}}$ which is due to the interaction of the incident and reflected electromagnetic waves,

$$\mathbf{J}_{2\omega} = \frac{e^3}{2im^2\omega^3} (\mathbf{E}_0 \mathbf{E}_B^* + \mathbf{E}_0^* \mathbf{E}_B) \cdot \nabla n, \quad (1)$$

where \mathbf{E}_0 and \mathbf{E}_B are the fields of the incident and backscattered wave, respectively, and ∇n is the density gradient. As one can see a radial component of ∇n is needed to obtain 2ω emission at 90° . Strong gradients can be supplied by filamentation. The frequency of the 2ω field is then exactly $\omega_0 + \omega_B$ where ω_B is the frequency of the Brillouin backscattered wave, given by

$$\omega_B = \omega_0 \left[1 - 2 \frac{v_i}{c} \left[\frac{1 - n_e/n_c}{1 + 4k_0^2 \lambda_D^2 (n_e/n_c - 1)} \right]^{1/2} \right], \quad (2)$$

where $v_i = [(ZT_e + 3T_i)/m_i]^{1/2}$ is the speed of the ion-acoustic wave, \mathbf{k}_0 is the laser wave vector, and λ_D the

Debye length; T_e and T_i are the electron and ion temperature, respectively, in energy units. Our data are consistent with this explanation provided one takes into account that

$$\frac{\Delta\omega}{\omega} \bigg|_{2\omega_0} = \frac{1}{2} \frac{\Delta\omega}{\omega} \bigg|_{\omega_0} \quad (3)$$

Figure 3 shows that the initial position of the 2ω line [trace (1)] has a red shift $\Delta\lambda \approx 4 \text{ \AA}$ corresponding to $v_i = 2.5 \times 10^7 \text{ cm sec}^{-1}$, i.e., $T_e \approx T_i \approx 600 \text{ eV}$. This temperature is expected in the given experimental condition and is roughly constant in time after burnthrough,¹⁰ i.e., during the peak of the laser pulse, when most 2ω is emitted.

The increase in red shift observed during the emission is explainable in terms of Doppler shift due to the plasma motion in the direction of the beam axis (parallel to \mathbf{k}_0). This motion is accelerated due to both ablation and light pressure. From the red shift at 2ω the velocity v_p of the plasma motion can be evaluated if we put in Eq. (2) $v_i + v_p$ in place of v_i , taking $v_i = 2.5 \times 10^7 \text{ cm sec}^{-1}$. For all the spectra obtained with 1–1.5- μm targets we find $v_p \approx 2 \times 10^7 \text{ cm sec}^{-1}$ at delays of a few hundred picoseconds, up to $v_p \approx 6 \times 10^7 \text{ cm sec}^{-1}$ after $\approx 2 \text{ ns}$. These velocities are reasonable in our experimental condition and are comparable with other experimental data.¹¹

The 2ω line bandwidth showed a net increase during the emission, typically from 5 \AA to about 20 \AA . It is a consequence of the increasing bandwidth of the electromagnetic wave backscattered by the Brillouin process. Landau damping of ion sound waves¹² could be in principle responsible for line broadening, but calculation leads to a narrower bandwidth than observed. We believe that the line bandwidth is essentially due to Doppler broadening related to plasma expansion. Consequently, the doublet structure apparent in most late-time spikes (for example, at 1.8 ns in Fig. 3) should indicate that two plasma regions with different velocities are more effective in SBS (and consequent sum-frequency generation). Let's assume that these two regions have opposite velocities $\pm v_{\text{rel}}$ relative to the plasma center of mass. We can evaluate v_{rel} from the doublet separation; the trace (4) of Fig. 3 gives $v_{\text{rel}} \approx v_i$: The sonic layers of the expanding plasma seem the most involved in the emission process.

We also expect that filamentation of the laser beam plays a role in the side emission of 2ω , as already observed:⁹ Filamentation can be responsible for density gradient formation and also for an extra heating which can contribute to the increasing red shift observed in this experiment. Evidence of such an extra heating in SBS spectra has been recently reported from an experiment in preformed plasmas.¹³ This effect can contribute as well to the shaping of our spectra. However, a pure filamentation effect cannot explain the observed red shift because it requires filament temperatures up to several

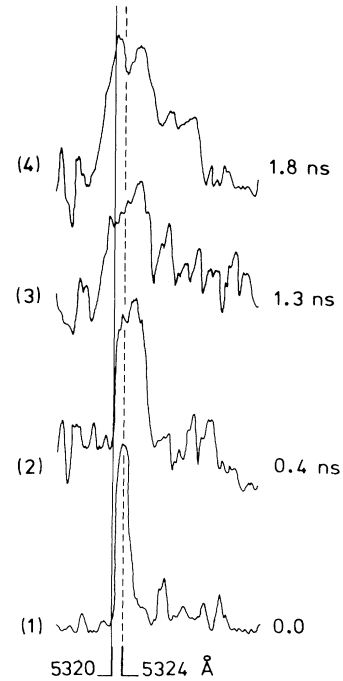


FIG. 3. Densitometer traces from spectrum *b* of Fig. 1 at different delays with respect to the starting time of the 2ω emission. *Solid line*: Exact second-harmonic wavelength. *Dashed line*: Wavelength position given by Brillouin shift corresponding to $T_e = T_i = 600 \text{ eV}$.

keV.

In conclusion, we obtained time-resolved spectra and time-resolved images of the 2ω emission perpendicular to the beam axis in an underdense plasma. The spectroscopic data are consistent with second-harmonic emission resulting from the sum of the laser frequency with the frequency of the backscattered light. The signature of this process comes from the red shift of the backscattered light as expected from SBS which in turn gives a red shift of the second-harmonic light. Other spectroscopic features are explainable in terms of the plasma motion. In addition, the measured threshold of the 2ω emission agrees with the expected SBS threshold in our experimental conditions.

The frequency sum process, postulated by Stamper *et al.*⁹ is now experimentally confirmed as a nonlinear process occurring in laser-produced plasmas as well as already observed in crystals.¹⁴ The emission detected in this experiment can be used, in principle, as a diagnostic in place of direct measurements on stimulated Brillouin backscattered light. A disadvantage is given by equality (3) making the spectroscopic analysis less sensitive. However, this method could be convenient because 2ω light is spectroscopically well separated from the fundamental ω_0 much better than ω_B . Moreover, the experimental detection is generally more suitable at 90° than

backward.

The authors are grateful to E. Fabre and C. Labaune for enlightening discussions; the contribution of I. Deha and the technical support of S. Bartalini were important to the success of this work. This work was fully supported by Consiglio Nazionale delle Ricerche, Italy.

^(a)Also at Dipartimento di Fisica, Università di Pisa, Pisa, Italy.

¹H. J. Herbst *et al.*, Phys. Rev. Lett. **46**, 328 (1981).

²N. G. Basov *et al.*, in *Heating and Compression of Thermonuclear Targets by Laser Beam*, edited by N. G. Basov (Cambridge Univ. Press, Cambridge, 1986).

³Gu Min and Tan Weihan, Laser Part. Beams **6**, 569 (1988), and references therein.

⁴S. Jackel, B. Perry, and M. Lubin, Phys. Rev. Lett. **37**, 95 (1976).

⁵Gu Min *et al.*, Phys. Fluids **30**, 1515 (1987).

⁶D. Batani *et al.*, Opt. Commun. **70**, 38 (1989).

⁷D. Giulietti *et al.*, Laser Part. Beams **6**, 141 (1988).

⁸I. V. Alexandrova *et al.*, Pis'ma Zh. Eksp. Teor. Fiz. **38**, 478 (1983) [JETP Lett. **38**, 577 (1983)].

⁹J. A. Stamper *et al.*, Phys. Fluids **28**, 2563 (1985).

¹⁰R. A. London and M. D. Rosen, Phys. Fluids **29**, 3813 (1986).

¹¹K. Eidmann *et al.*, Phys. Rev. A **30**, 2568 (1984).

¹²T. P. Hughes, in *Laser-Plasma Interactions*, edited by R. A. Cairns and J. J. Sanderson (SUSSP Publications, Edinburgh, 1980), p. 10.

¹³O. Willi *et al.*, Opt. Commun. **70**, 6 (1989).

¹⁴Y. R. Shen, *The Principles of Nonlinear Optics* (Wiley, New York, 1984).

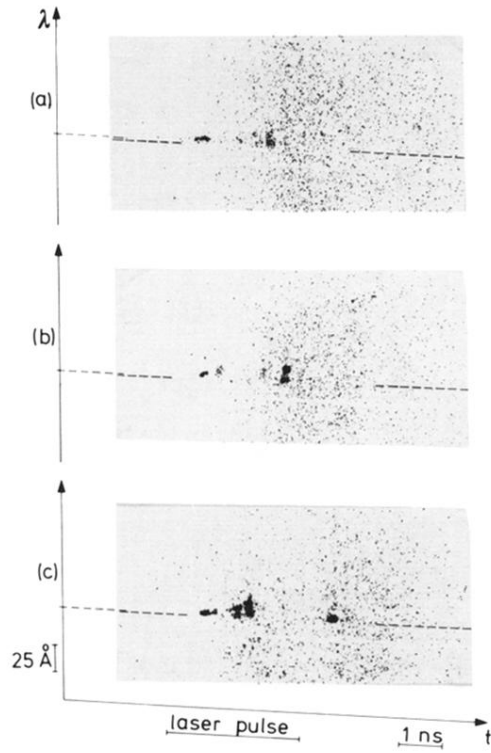


FIG. 1. Time-resolved spectra of 2ω emission. (a) Shot No. 211207: Intensity $I=1.2\times 10^{13}$ W/cm 2 , target thickness $d=1.58$ μ m; (b) No. 211209: $I=1.4\times 10^{13}$ W/cm 2 , $d=1.58$ μ m; (c) No. 231204: $I=1.5\times 10^{13}$ W/cm 2 , $d=1.50$ μ m. Contrast was enhanced by photographic processing to evidence structures. The “laser pulse” bar refers to the FWHM duration and roughly matches the pulse timing. Dashed lines indicate the wavelength position of the exact $2\omega_0$.

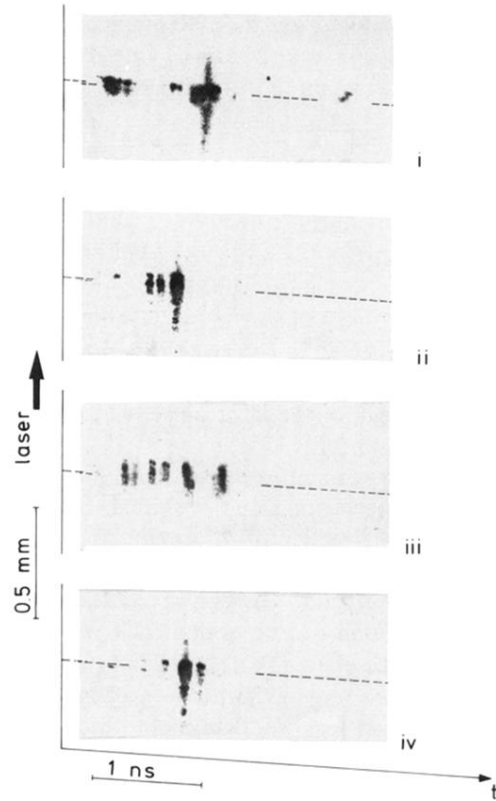


FIG. 2. Time-resolved images of 2ω sources. (i) No. 070202: $I=1.3\times 10^{13}$ W/cm², $d=1.56$ μ m; (ii) No. 060204: $I=1.5\times 10^{13}$ W/cm², $d=1.39$ μ m; (iii) No. 060209: $I=1.5\times 10^{13}$ W/cm², $d=1.39$ μ m; (iv) No. 211209: $I=1.7\times 10^{13}$ W/cm², $d=1.21$ μ m. Contrast was enhanced by photographic processing to show structures. The initial target plane position is approximately indicated by dashed lines.